Wave chaos for the Helmholtz equation

Olivier Legrand, Fabrice Mortessagne

Wave chaos for the Helmholtz equation

O. Legrand and F. Mortessagne
Laboratoire de Physique de la Matière Condensée
CNRS - UMR 6622
Université de Nice-Sophia Antipolis
Parc Valrose F-06108 Nice Cedex 2 FRANCE

I. INTRODUCTION

The study of wave propagation in complicated structures can be achieved in the high frequency (or small wavelength) limit by considering the dynamics of rays. The complexity of wave media can be either due to the presence of inhomogeneities (scattering centers) of the wave velocity, or to the geometry of boundaries enclosing a homogeneous medium. It is the latter case that was originally addressed by the field of *Quantum Chaos* to describe solutions of the Schrödinger equation when the classical limit displays chaos. The Helmholtz equation is the strict formal analog of the Schrödinger equation for electromagnetic or acoustic waves, the geometrical limit of rays being equivalent to the classical limit of particle motion. To qualify this context, the new expression *Wave Chaos* has naturally emerged. Accordingly, *billiards* have become geometrical paradigms of wave cavities.

In this chapter we will particularly discuss how the global knowledge about ray dynamics in a chaotic billiard may be used to explain universal statistical features of the corresponding wave cavity, concerning spatial wave patterns of modes, as well as frequency spectra. These features are for instance embodied in notions such as the *spatial ergodicity* of modes and the *spectral rigidity*, which are indicators of particular spatial and spectral correlations. The spectral study can be done through the so-called *trace formula* based on the *periodic orbits* of chaotic billiards. From the latter we will derive universal spatial and spectral features in agreement with predictions of *Random Matrix Theories*, but also see that actual deviations from a universal behavior can be found, which carry information about the specific geometry of the cavity. Finally, as a first step towards disordered scattering systems, a description of spectra of cavities dressed with a point scatterer, will be given in terms of *diffractive orbits*.

II. RAY CHAOS AND TRACE FORMULA FOR THE HELMHOLTZ EQUATION

A. Ray chaos in cavities - Periodic Orbits

The Helmholtz equation describes a variety of stationary wave-phenomena studied in electro-magnetism, acoustics, seismology and quantum mechanics; its general form for a (complex) scalar wavefunction ψ (ψ being the pressure variation in a fluid, a component of the electromagnetic field in a cavity, the elevation of a membrane, ...) reads

$$\left(\vec{\nabla}^2 + k^2(\vec{r})\right)\psi(\vec{r}) = 0 \tag{1}$$

The wavenumber k depends explicitly on space according to the dispersion relation $k^2(\vec{r}) = \omega^2/c^2(\vec{r})$, where $c(\vec{r})$ is the spatially varying wave velocity. By writing the wavefunction in the form $\psi(\vec{r}) = A(\vec{r})\exp\left[\mathrm{i}S(\vec{r})\right]$, and by neglecting term of the form $\vec{\nabla}^2 A/A$, equation (1) leads to the so-called Eikonal equation for the phase

$$\left(\vec{\nabla}S\right)^2 = k^2(\vec{r}) \tag{2}$$

In the geometrical limit, the rays may be viewed as the characteristic curves $[\vec{r}(t), \vec{k}(t)]$ of a fictitious particle of variable mass $(2c^2)^{-1}$ and pseudo-momentum $\vec{k}$ whose dynamics is controlled by the Hamiltonian [1]

$$H(\vec{r}, \vec{k}) = c^2(\vec{r})\vec{k}^{\,2} = \omega^2 \tag{3}$$

The ray trajectories are given by the Hamilton's equations of motion:

$$\frac{\mathrm{d}}{\mathrm{d}t}\vec{r} = \frac{c^2}{\omega}\vec{k}, \qquad \frac{\mathrm{d}}{\mathrm{d}t}\vec{k} = -\frac{c}{\omega}k^2\vec{\nabla}c = -\frac{\omega}{c}\vec{\nabla}c \tag{4}$$

Acoustic enclosures or rooms are common examples of complex wave cavities where the dynamics of rays may generically display chaos. Using the formal analogy between the geometrical limit of rays and classical mechanics,

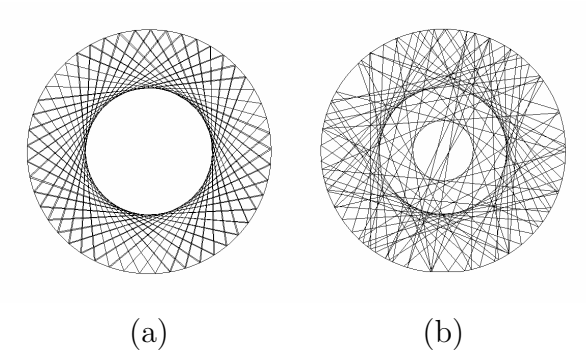

FIG. 1: Examples of a single ray trajectory after a propagation of 150 in units of the radius R: (a) inside a circular billiard, where a caustic is clearly observed; (b) inside a circular billiard cut by a small straight segment of length $10^{-2}R$. The caustic is destroyed due to the chaotic motion.

the simplest paradigms of such enclosures are *billiards*, which are closed homogeneous domains containing a particle specularly bouncing on the walls. According to the shape of the billiard, the motion may be regular or chaotic. Without going into too technical details, we wish now to illustrate the particular dynamics of chaotic billiards. Let us first recall the regular motion of rays in the billiard with the shape of a circle. The Fig. 1 (a) shows a typical trajectory within such a billiard after a propagation length of 150 in units of the radius R. One can clearly observe the presence of a caustic. The latter encloses a region of space that this trajectory never visits (whatever the number of reflections). This kind of structure is destroyed in chaotic billiards. This is exemplified by considering the following modification of the previous billiard. A new shape is obtained by cutting a small straight segment of length $10^{-2}\,R$. Whereas the change of boundary is not visible on Fig. 1 (b), its effect on the dynamics is dramatic: for the same initial conditions (position and direction) the formerly forbidden region is invaded after a finite number of reflections. In the theory of Hamiltonian chaos, it is shown that this effect stems from the *extreme sensitivity to initial conditions*, which appears for any non-vanishing size of the cut (except for a cut of length $2R$ which corresponds to the semi-circle billiard).

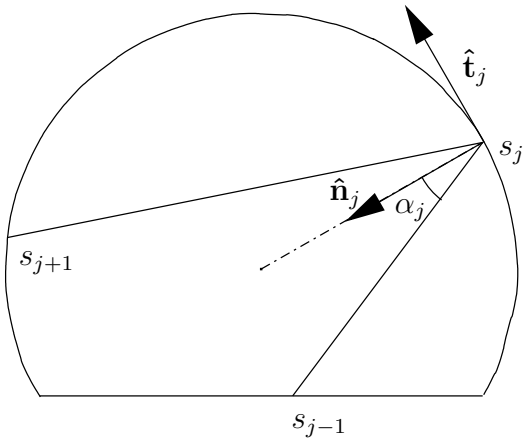

FIG. 2: Representation of the dynamics in a billiard through the coordinates associated, at each rebound, to the curvilinear abscissa s along the boundary, and the sine of the angle of reflection α with respect to the inward boundary normal.

The qualification of chaos is more conveniently studied through a phase space representation. A common representation in billiards consists in restricting the dynamics to the knowledge, at each impact, of the curvilinear abscissa, s, and of the sine of the angle of reflection, α, with respect to the inward boundary normal (see Fig. 2). Thus, at jth reflection, defining $\hat{\mathbf{t}}_j$ the unit vector tangent to the oriented boundary at abscissa s_j, and $\hat{\mathbf{n}}_j$ the inward normal unit vector, the pseudo momentum reads $\vec{k} = \sin\alpha_j\hat{\mathbf{t}}_j + \cos\alpha_j\hat{\mathbf{n}}_j$. The same trajectories as in Fig. 1, are shown in the phase space $(s, \sin\alpha)$ on Fig. 3 for a finite number of bounces: the regular motion is associated to the conservation of α in the circular billiard (Fig. 3 (a)), while in the truncated billiard, which is chaotic, the whole phase space is

eventually uniformly covered by almost any trajectory (Fig. 3 (b)). It should be mentioned here that there exist particular trajectories which do not fit into this scheme, namely, the periodic orbits. These orbits are trajectories which close upon themselves in phase space (hence also in real space). For a chaotic system they must, of course, be unstable in the sense that any small initial deviation from it must diverge exponentially with time.

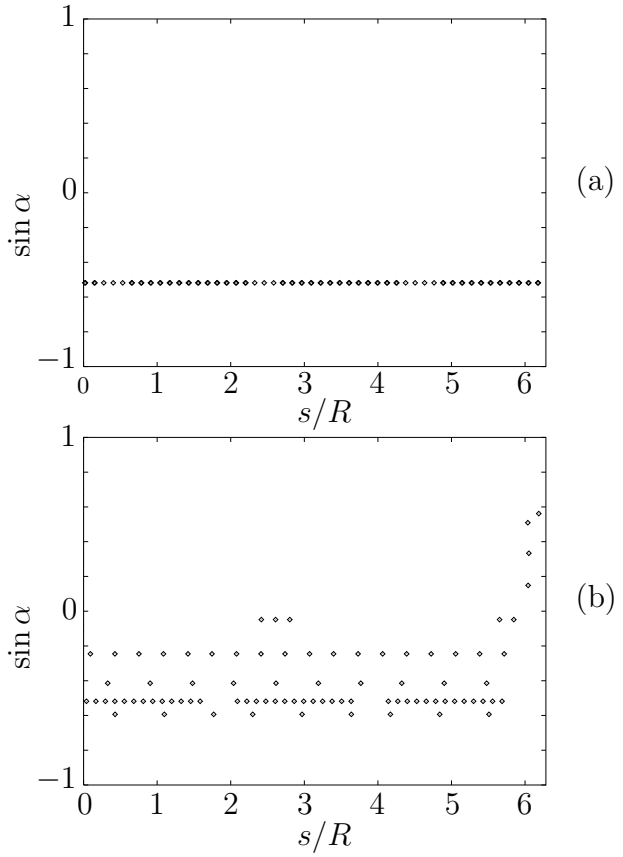

FIG. 3: Same trajectories as in figure 1 using the phase space coordinates $(s, \sin\alpha)$ introduced in figure 2. (a) The regular motion in the circular billiard is associated to the conservation of α, (b) while, in the chaotic billiard, the whole phase space is asymptotically uniformly covered by almost any ray trajectory.

It is important to stress here that if one considers rays as trajectories of pointlike particles carrying wave energy, then the assumption of uniform and isotropic distribution of wave energy, commonly used in reverberant enclosures, is fulfilled in chaotic billiards. This is the basis for all exponential reverberation laws used in room acoustics since the pioneering works of Sabine (see for instance [2, 3] and references therein).

B. The Semiclassical approach for Chaotic Systems - The Trace formula

The aim of a semiclassical (high-frequency) analysis is to obtain approximate solutions for the response of the stationary wave equation, only by means of classical trajectories and the wavelength λ when the latter can be assumed to be small enough compared to all sizes of the billiard. In the following, we will be interested in homogeneous media where the Helmholtz scalar wave equation holds :

$$(\vec{\nabla}^2 + k^2)\psi(\vec{r}) = 0 \quad \text{inside the enclosure} \quad \mathcal{D} \tag{5}$$

where $k = 2\pi/\lambda$ is the wavenumber which can only take on discrete values, due to the Dirichlet conditions $\psi = 0$ prescribed at the boundary $\partial\mathcal{D}$ of the enclosure. Other boundary conditions would also produce a discrete spectrum of values for k as long as they correspond to lossless conditions.

The eigenfunctions ϕ_n of this boundary-value problem form a complete set enabling the following expansion for the

Green's function of equation (5) :

$$G(\vec{r}_B, \vec{r}_A; k) = \sum_n \frac{\phi_n^*(\vec{r}_B)\phi_n(\vec{r}_A)}{k^2 - k_n^2}\,. \tag{6}$$

In the limit $k|\vec{r}_B - \vec{r}_A| \gg 1$, the Green's function can be approximated as a sum over all geometrical ray contributions from multiply reflected trajectories connecting points A and B (the so-called semiclassical Green's function; see for instance [4] or [5])

$$G_{sc}(\vec{r}_B, \vec{r}_A; k) = \sum_{q\,,\ \mathrm{A}\,\to\,\mathrm{B}} \frac{1}{\mathrm{i}(2\pi i)^{(d-1)/2}} \left|\Delta_{AB,q}\right|^{1/2} \exp\left[\mathrm{i}S_q(\vec{r}_B, \vec{r}_A; k) - \mathrm{i}\frac{\pi}{2}m_q\right]\,. \tag{7}$$

where the *action* $S_q = kL_q$ is proportional to the path length $L_q(\vec{r}_B, \vec{r}_A)$ along the trajectory labeled q, and $m_q = 2n_{r,q} + n_{c,q}$ is the so-called Maslov index, with $n_{r,q}$ and $n_{c,q}$ denoting the number of reflections at the boundary and the number of passages through caustics. The *divergence* factor Δ_{AB} has the following geometrical expression

$$\Delta_{AB} = \frac{k^{(d-3)}}{4}\frac{\mathrm{d}\Omega_A}{\mathrm{d}A_B} \tag{8}$$

where $\mathrm{d}A_B$ is the $(d-1)$-dimensional cross section at point B of the tube of rays starting from A within a solid angle $\mathrm{d}\Omega_A$ in the vicinity of a given trajectory.

To fix ideas, in the 2D case, for a direct trajectory without reflection between A and B, $|\mathrm{d}\Omega_A/\mathrm{d}A_B|^{1/2}$ reduces to $1/\sqrt{L_q}$ whereas, after many reflections, in a chaotic billiard, it will typically decrease like $\exp(-hL_q/2)$ where h is the instability rate per unit length (Lyapunov exponent).

To retrieve some information about the frequency spectrum and the eigenfunctions from this asymptotic approach one needs a more global quantity than the Green's function itself. The expected connection between ray and modal spectral properties can be deduced from the so-called trace formula. Let us briefly describe its derivation from the above expression (7). First, one needs to handle the pole singularities in (6) by using

$$\frac{1}{k^2 - k_n^2} \to \lim_{\varepsilon\to 0^+} \frac{1}{(k^2 + i\varepsilon) - k_n^2} = \mathcal{P}\left(\frac{1}{k^2 - k_n^2}\right) - i\pi\delta(k^2 - k_n^2)\,, \tag{9}$$

where $\mathcal{P}(\cdot)$ denotes the Cauchy principal value. Relation (9) implies that the imaginary part of the Green's function, once integrated over the domain (often referred to as a *trace* in quantum physics), yields the density of eigenvalues :

$$\frac{1}{\pi}\mathrm{Im}\left[\int_{\mathcal{D}} G(\vec{r}, \vec{r}; k)\mathrm{d}\vec{r}\right] = \sum_n \delta(k^2 - k_n^2)\,. \tag{10}$$

This quantity represents the eigenvalue-density function $D(k^2)$ in terms of the variable k^2 (also known as the density of states (DOS) in quantum physics) which is related to the modal density $\rho(k) = \sum_n \delta(k - k_n)$ through $\rho(k) = 2kD(k^2)$.

In the high-frequency limit, if one uses the semiclassical approximation (7) in the above equation, one notices the rapidly oscillating factor $\exp[ikL_q]$. One can therefore evaluate the spatial integral by stationary phase. Indeed, the equations of motion for the ray trajectory from A to B imply that the partial derivative of $L_q(\vec{r}_B, \vec{r}_A)$ with respect to $\vec{r}_B$ is the unit vector $\hat{n}_B$ tangent to the trajectory at B while its derivative with respect to $\vec{r}_A$ is minus the unit vector $\hat{n}_A$ tangent to the trajectory at A. Thus, the stationary-phase condition imposed at $\vec{r} = \vec{r}_B = \vec{r}_A$ selects closed trajectories in phase space, i.e. *periodic orbits*. All this finally yields the celebrated trace formula over periodic orbits (PO), also known as the Gutzwiller trace formula [4]:

$$\rho(k) = \overline{\rho}(k) + \frac{1}{\pi}\sum_{\mathrm{pPO}\,q} L_q \sum_{\mathrm{repetitions}\,r} \frac{\cos\left[r(kL_q - m_q\pi/2)\right]}{\left|\det\left(1 - M_q^r\right)\right|^{1/2}}\,, \tag{11}$$

where the summation is performed over all primitive periodic orbits (pPO) and their repetitions, and M_q is the monodromy matrix of the pPO describing the linear change of the transverse coordinates (in phase space) after one period.

In formula (11), $\overline{\rho}(k)$ is the contribution of the *zero-length* trajectories. For such trajectories, the semiclassical approximation is not valid and the space integral must be performed by using the free-space Green's function:

$$\overline{\rho}(k) = \frac{2k}{\pi}\mathrm{Im}\left[\int_D \lim_{\vec{r}_B\to\vec{r}_A} G_0(\vec{r}_B, \vec{r}_A; k)\mathrm{d}\vec{r}_A\right] \tag{12}$$

This corresponds to the average behavior of the modal density, varying smoothly with k, and given, in billiards, by an asymptotic series in powers of k^{-1} whose leading term is known as the Weyl's law (also known as the Thomas-Fermi approximation in nuclear physics) and reads:

$$\rho_{Weyl}(k) = \frac{V_d \Omega_d}{(2\pi)^d} k^{d-1} \,. \tag{13}$$

where V_d is the d-dimensional volume of the billiard and Ω_d is the surface of the d-dimensional sphere of unit radius. The sum over periodic orbits describes the oscillatory behavior, denoted ρ^{osc}, of this density around its smooth component. Longer periodic orbits contribute to finer oscillations and the largest length required to describe the modal density at the scale of the mean spacing $1/\overline{\rho}(k)$ is called the Heisenberg length $L_H(k) \equiv 2\pi\overline{\rho}(k)$. For periodic orbits longer than L_H, as noted by Bogomolny and Keating [6], their contributions should not provide any significant information about the modal density other than to account for the discreteness of the spectrum: this implies subtle compensations between terms indicating in fact that most of the information contained in long orbits can be retrieved from shorter ones. We will come back to this point later in the section devoted to the spectral correlations. Note that formula (11) is only valid at the lowest order in the small parameter $(kL)^{-1}$, where L is a typical size of the billiard, and also that it should be restricted to isolated orbits which is typically the case in truly chaotic billiards. In the case of continuous families of orbits, especially for integrable billiards, a sum over periodic orbits can be analytically performed through the use of Poisson sum rules (see e.g. [7], chap. 7 section 1, or also [8, 9]). Another related problem is the apparent lack of convergence of the Trace formula in chaotic billiards. Indeed, long orbits have amplitudes behaving like $L_q \exp(-hL_q/2)$, while it is known that the number of periodic orbits with period less that L proliferates like $(hL)^{-1}\exp(hL)$ [10]. This should imply that the sum does not converge unless, as already mentioned above, the fact that the POs are not independent and that the information they contain is structured, conspire in such a way to ensure convergence.

C. Speckle-like and Scarred Wavefunctions

The chaotic exploration of phase space by rays illustrated in section II A should be expected to govern the statistical spatial distribution of eigenmodes. Such an ergodic behavior was, indeed, rigorously demonstrated in the late 70's by Voros [11] and popularized by Berry [12] through an analogy with laser speckle patterns. Berry provided evidence that the wavefunction of a typical mode may be viewed as a Gaussian random function resulting from a random superposition of plane waves [13]. The ergodicity of eigenmodes emerges through the normalized local density of states defines as follows

$$\tilde{\rho}(\vec{r},\omega^2) = \frac{\int \mathrm{d}\vec{k}\,'\,\delta\big(\omega^2 - H(\vec{r},\vec{k}\,')\big)}{\int \mathrm{d}\vec{r}\,'\mathrm{d}\vec{k}\,'\,\delta\big(\omega^2 - H(\vec{r}\,',\vec{k}\,')\big)} \tag{14}$$

where $H(\vec{r},\vec{k})$ is the Hamiltonian given in (3). In the semiclassical limit $kL \to \infty$ equation (14) turns into

$$\tilde{\rho}(\vec{r},\omega^2) \simeq \lim_{kL\to\infty} \big\langle |\psi(\vec{r})|^2 \big\rangle_{\omega^2} = \frac{1}{N}\sum_n |\phi_n(\vec{r})|^2 \tag{15}$$

where the sum runs over N eigenmodes centered on "energy" ω^2 (on wavenumber $k(\vec{r}) = \sqrt{\omega^2/c^2(\vec{r})}$, equivalently) in an interval small enough for the density of states to remain constant and large enough to ensure a large value of N. In practice, less and less modes are required as the central mode is far in the semiclassical domain, and, eventually, the ergodic behavior is obtained for individual modes. As an illustration, equation (5) has been numerically solved for a domain $\mathcal{D}$ with the shape of the chaotic billiard shown in figure 2. Recall that in the billiard case the velocity is uniform inside the domain: $c(\vec{r}) \equiv c$ and, consequently, $\omega^2 = c^2k^2$. In figure 4, the square amplitude of the mode number $n = 1513$ ($k_{1513} = 87.89\,R^{-1}$) is depicted. The ergodic nature of the mode is clearly shown: apart from the axial symmetry such an eigenmode can be viewed, locally, as a superposition of planes waves with fixed k and random phases and directions. As a consequence, the field autocorrelation function defined as follows

$$C_\psi(\vec{r},\vec{r}_0;k) = \big\langle \psi^*(\vec{r} - \tfrac{1}{2}\vec{r}_0)\psi(\vec{r} + \tfrac{1}{2}\vec{r}_0)\big\rangle_k \tag{16}$$

reads [12, 14]

$$C_\psi(\vec{r},\vec{r}_0;k) = \frac{\int \mathrm{d}\vec{k}\,' \,\exp\Big[\mathrm{i}\vec{k}\,'\cdot\vec{r}_0\Big]\,\delta\big(c^2k^2 - H(\vec{r},\vec{k}\,')\big)}{\int \mathrm{d}\vec{r}\,'\mathrm{d}\vec{k}\,'\,\delta\big(c^2k^2 - H(\vec{r}\,',\vec{k}\,')\big)} \tag{17}$$

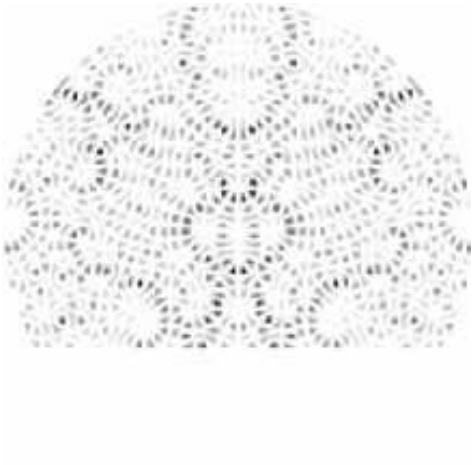

FIG. 4: A typical *ergodic* eigenmode (squared amplitude), solution of Eq. (5) with Dirichlet boundary conditions, in the truncated chaotic billiard with $k \times R = 87.89$. Apart from the obvious symmetry, such an eigenmode can be viewed as a superposition of plane waves at a given k with random phases and directions.

In a 2D billiard the Hamiltonian is uniform and in equation (17) the Dirac δ function only fixes the norm of $\vec{k}$ giving rise to the important result [12]

$$C_\psi(\vec{r}, \vec{r}_0; k) = J_0(kr_0) \tag{18}$$

where J_0 is the zeroth-order Bessel function and r_0 is the norm of $\vec{r}_0$. Using an ergodic hypothesis, the average in (16) can be replaced by a spatial average over the midpoint $\vec{r}$, which, in practice, should be evaluated over a domain encompassing a sufficiently large number of oscillations [14].

In the asymptotic limit, a random superposition of plane waves with random uncorrelated phases is expected to yield a Gaussian random field. In the case of real eigenmodes, this implies that the probability $P(\psi)\mathrm{d}\psi$ that the eigenfunction has a value between ψ and $\psi + \mathrm{d}\psi$ is given by

$$P(\psi) = \frac{1}{\sqrt{2\pi\langle\psi^2\rangle}} \exp\left(-\frac{\psi^2}{2\langle\psi^2\rangle}\right) . \tag{19}$$

where $\langle\cdots\rangle$ denotes a spatial average on the domain $\mathcal{D}$. One should note that a Gaussian distribution does not imply the stronger requirement (17). The result (19) is also recovered by Random Matrix Theory (RMT) for the Gaussian Orthogonal Ensemble of real symmetric $N \times N$ matrices in the limit $N \to \infty$ [15] (see also [16]). Indeed, RMT leads to the so-called Porter-Thomas distribution for the squared eigenvectors components. The latter distribution is obtained from (19) for the intensity $I = \psi^2$ and reads

$$P(I) = \frac{1}{\sqrt{2\pi I/\langle I\rangle}} \exp\left(-\frac{I}{2\langle I\rangle}\right) . \tag{20}$$

To check this behavior, we first numerically solve the Helmholtz equation (5) with Dirichlet boundary conditions using a plane wave decomposition method. This method [17] has allowed the calculation of the first 2 000 eigenmodes of the truncated circle billiard [18]. Because of Dirichlet boundary conditions, the eigenmodes are chosen to be real.

Using these calculated modes, we have evaluated the *radial* field autocorrelation function $C_\psi(r_0; k)$

$$C_\psi(r_0; k) = \frac{1}{2\pi} \int_0^{2\pi} \mathrm{d}\theta \, C_\psi(\vec{r}_0; k) \tag{21}$$

with θ the polar angle and where the field autocorrelation function $C_\psi(\vec{r}_0; k)$ is equivalent to (16) with a spatial average over $\vec{r}$

$$C_\psi(\vec{r}_0; k) = \left\langle \psi^\star(\vec{r} - \tfrac{1}{2}\vec{r}_0)\psi(\vec{r} + \tfrac{1}{2}\vec{r}_0)\right\rangle_{\vec{r}} \tag{22}$$

where the average $\langle \cdots \rangle_{\vec{r}}$ reads $\iint_{\mathcal{D}} \cdots \mathrm{d}\vec{r} / \iint_{\mathcal{D}} |\psi(\vec{r})|^2 \mathrm{d}\vec{r}$, with $\mathcal{D}$ the domain of integration.

In Fig. 5, we have represented one typical high energy eigenmode (amplitude) of the truncated circle billiard for a value of k equal to 87.89 in units of inverse radius R, its probability distribution and the corresponding radial field autocorrelation function following Eqs. (21) and (22). The assumption of a random superposition of plane waves is confirmed by the good agreement between the probability distribution $P(\psi)$ and the Gaussian distribution as can be seen in Fig. 5 (b). The radial autocorrelation function $C_\psi(r_0; k)$ is compared to the expected zero order Bessel function $J_0(kr_0)$ for $k \times R = 87.89$. Note that the prediction (18) is perfectly verified.

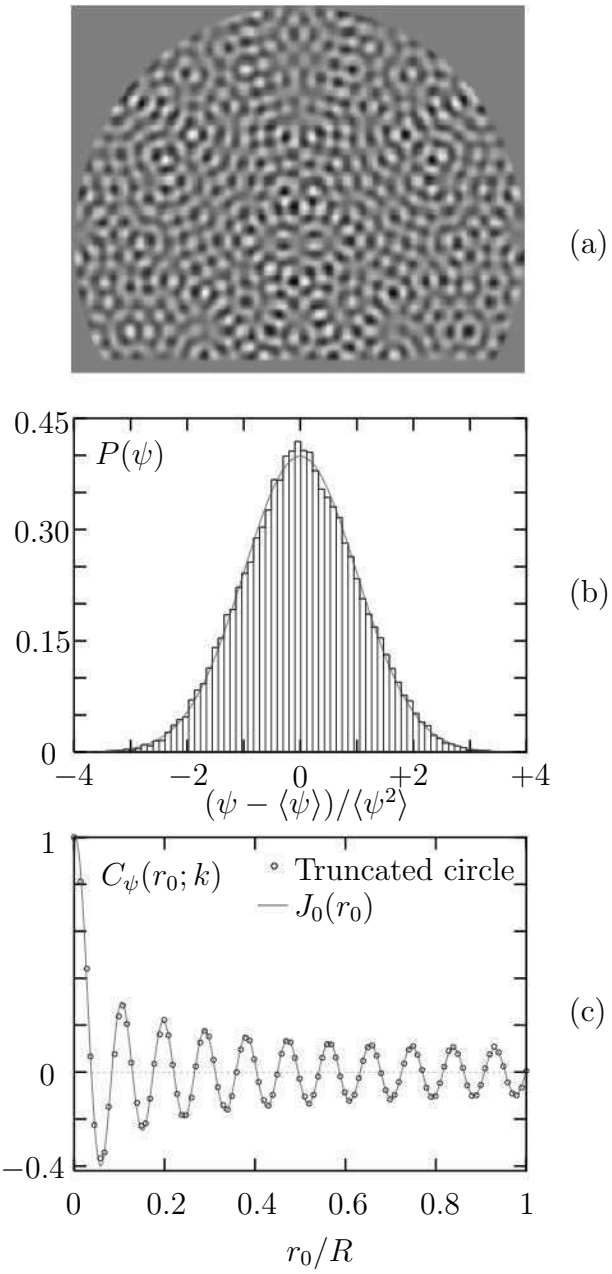

FIG. 5: (a) A high energy eigenmode (amplitude) with $k \times R = 87.89$ in the truncated chaotic billiard, (b) its associated probability distribution $P(\psi)$, compared to a Gaussian distribution (continuous line), and (c) the radial field autocorrelation function $C_\psi(r_0; k)$.

As any prediction concerning average behaviors, the results presented just above suffer rare but important exceptions. Indeed, inspecting Fig. 6 (a), a clear deviation from ergodicity is seen, which is in fact associated to a particular periodic orbit (superimposed as a solid line). This intensity enhancement in the vicinity of a single periodic

orbit is coined *scarring* [17, 19]. This unexpected behavior has led the Quantum Chaos community to reconsider the semiclassical limit (14). They have established that the semiclassical skeleton of eigenmodes is built on all the periodic orbits of the system. Thus the one-to-one relationship shown in Fig. 6, between an eigenmode and a periodic orbit, has to be considered as an exception, since, as the number of POs proliferates exponentially with their lengths, eigenmodes must build upon many of them. A thorough description of the subtle scarring phenomenon is given by E. Vergini in the present book [20].

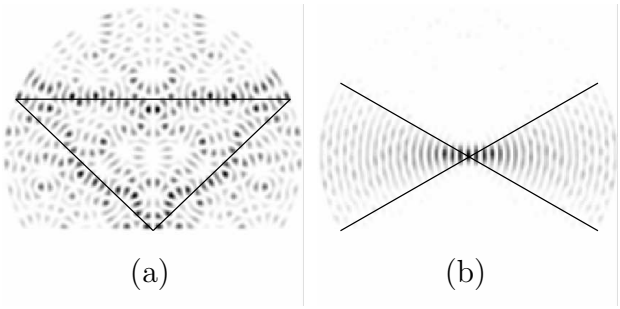

FIG. 6: Examples of eigenmodes displaying an intensity enhancement in the vicinity of (a) an unstable periodic orbit (superimposed as a solid line), (b) the continuous family of diameters (boundaries shown as solid lines).

III. TWO-POINT SPECTRAL CORRELATIONS AND FORM FACTOR (SPACE-AVERAGED TIME-RESPONSE)

A. Spectral Rigidity à la Berry (diagonal approximation)

1. Form Factor

In a complex wave system, either a chaotic cavity or a disordered medium, it is not possible to give a detailed description of the frequency spectrum by providing a determined sequence of numbers. Hence, the frequency spectrum is too complicated to be explained level by level but may nevertheless be studied through a statistical approach, in a way quite analog to the statistical approach of a gas of interacting particles. In the study of spectral properties, a key role is played by the spectral *correlations* and their description in terms of adequate quantities will be our concern in this section. With these quantities we will be in a position to establish how certain universal features predicted by RMT can be recovered from a global knowledge of chaotic dynamics but also in what respect some non-universal behavior can be related to the shortest POs of the system.

The spectral autocorrelation function $C_k(\kappa)$ of the modal density is defined in terms of the oscillating part ρ^{osc} of the modal density as

$$C_k(\kappa) = \langle \rho^{osc}(k+\frac{\kappa}{2})\rho^{osc}(k-\frac{\kappa}{2})\rangle_k \,. \tag{23}$$

where the brackets denote local averaging over k (in practice over an interval large enough to include a large number of eigenvalues but sufficiently small as to keep the modal density approximately constant). As $\rho^{osc} = \sum_n \delta(k-k_n) - \overline{\rho}$, it is quite easy to show (see e.g. [7]) that $C_\rho(\kappa)$ presents a δ-like behavior at the origin which can be accounted for by defining an ancillary quantity called the two-level cluster function $Y_2(\kappa)$ through

$$C_k(\kappa) = \overline{\rho}^2 \left[\delta\left(\kappa L_H\right) - Y_2\left(\kappa L_H\right)\right] \tag{24}$$

For the following calculations, it is convenient to re-write the trace formula for ρ^{osc} as

$$\rho^{osc}(k) = \sum_{\mathrm{PO}\, j} A_j \mathrm{e}^{\mathrm{i}kL_j} \,, \tag{25}$$

where the sum runs over all POs including repetitions and complex conjugate terms, stability and phase factors being integrated into the amplitudes A_j. The form factor is defined through the Fourier transform of the two-point

autocorrelation function $C_k(k)$ as

$$K(L) = \frac{1}{\overline{\rho}(k)} \int C_k(\kappa) \exp(\mathrm{i}\kappa L)\, \mathrm{d}\kappa \tag{26a}$$

$$= 1 - \frac{1}{2\pi} \int Y_2(s) \exp\left(\mathrm{i}s \frac{L}{L_H}\right) \mathrm{d}s \equiv 1 - b\left(\frac{L}{L_H}\right) , \tag{26b}$$

which, using (25), becomes

$$K_{sc}(L) = \frac{2\pi}{\overline{\rho}(k)} \sum_{jl} A_j^* A_l \mathrm{e}^{\mathrm{i}k(L_l - L_j)} \delta\left[L - \left(\frac{L_j + L_l}{2}\right)\right] . \tag{27}$$

For very short lengths (L of the order of the length of the shortest PO), $K(L)$ displays a series of sharp peaks. At longer lengths, due to the proliferation of POs, the peaks tend to overlap and one can try to evaluate the smooth behavior of the form factor by means of a classical sum rule. For large k, the terms of expression (27) with $L_j \neq L_l$ rapidly oscillate and cancel out in the process of averaging over a k-interval as mentioned above. This leads one to ignore all the off-diagonal terms of the sum, and, in this *diagonal* approximation, one is left with the following expression

$$K_{sc}^{diag}(L) = \frac{2\pi}{\overline{\rho}(k)} \sum_j |A_j|^2 \delta\left(L - L_j\right) . \tag{28}$$

For the pPOs, the squared modulus of the amplitude behaves like $|A_j|^2 \simeq \left(\frac{L_j}{2\pi}\right)^2 \exp(-hL_j)$ while their density (number of pPOs with period between L and $L+\mathrm{d}L$ over $\mathrm{d}L$) increases as $\exp(hL)/L$. Thus, ignoring the contributions of the repetitions of smaller orbits at a given lengths, one finally obtains

$$K_{sc}^{diag}(L) = \frac{L}{L_H} . \tag{29}$$

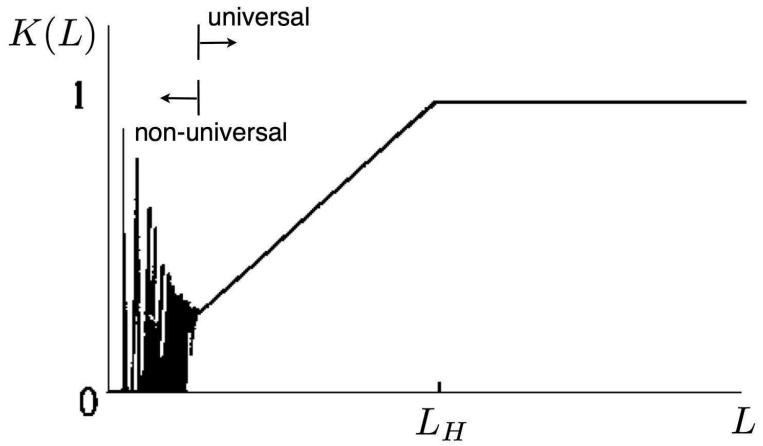

FIG. 7: Schematic representation of the semiclassical form factor, illustrating how the diagonal approximation predicts a non universal part showing peaks due to short POs and a universal part due to long POs but for lengths shorter than L_H. The unit value for $L \gg L_H$ is predicted by semiclassical arguments beyond the diagonal approximation

Of course, such an expression becomes unphysical for arbitrary long lengths and cannot be valid for $L \gtrsim L_H$. Indeed, for such long periods, a complete cancellation of non-diagonal terms cannot be achieved due to the increasing

number of POs whose lengths nearly coincide. Delande has proposed another semiclassical *sum rule* [21] which shows that

$$K_{sc}(L) \to 1 \text{ when } L \gg L_H \,. \tag{30}$$

The argument goes as follows. If the integral defining $K(L)$ is performed over an interval Δk containing $N = \overline{\rho}(k)\Delta k$ eigenvalues, it approximately reads (using the Wiener-Khinchin theorem) :

$$K(L) = \frac{1}{N}\left|\int_{k-\Delta k/2}^{k+\Delta k/2} [\rho(k') - \overline{\rho}(k')]\mathrm{e}^{-\mathrm{i}k'L}\mathrm{d}k'\right|^2 \tag{31a}$$

$$\approx \frac{1}{N}\left|\sum_n \exp(-\mathrm{i}k_n L)\right|^2 . \tag{31b}$$

At long lengths $L \gg L_H$, the oscillating terms in the above expression add incoherently, therefore yielding the limit (30). All the above results concerning the form factor are summarized in Fig. 7.

For time-reversal invariant systems, which is generally the case for classical wave cavities, one has to correct the preceding argument because, for each PO, there is a time-reverse PO with an identical amplitude and phase. Therefore, the corresponding off-diagonal terms in the double sum contribute the same amount as the diagonal terms, yielding a result that is doubled. At short times, expression (29) thus becomes

$$K_{sc}^{diag}(L) = 2\frac{L}{L_H} \,. \tag{32}$$

This turns out to be the result predicted by RMT in the case of the Gaussian Orthogonal Ensemble (see e.g. [16] or [15]) for which

$$b(x) = 1 - 2x + x\ln(1+2x) \quad \text{if} \quad 0 < x < 1 \tag{33a}$$

$$= -1 + x\ln\left[(2x+1)/(2x-1)\right] \quad \text{if} \quad x > 1 \,. \tag{33b}$$

The small-x and large-x behaviors of $b(x)$ perfectly agree with the above semiclassical predictions. That semiclassics and RMT agree about the universal behavior of the two-point spectral correlations is not a complete confirmation of the Bohigas-Giannoni-Schmit conjecture [22] which states that the spectral fluctuations of classically chaotic systems should be described by the relevant ensembles of random matrices. For example the nearest-neighbor spacing distributions derived form RMT have never been totally justified on semiclassical arguments. As has been shown with different classes of pseudo-integrable systems (see below the billiards with point scatterers), non-chaotic systems can very well mimic level repulsion or short range spectral rigidity. Thus a clear-cut separation between classically integrable or chaotic systems on the basis of their spectral properties is no longer really an issue.

2. Length Spectrum

In the non-universal regime corresponding to the lengths of the shortest POs, expression (28) can also be re-written as the squared modulus of the Fourier transform of expression (25) for ρ_{osc}. When restricting the integral to the neighborhood of a given k, $K_{sc}(L)$ can be written as

$$K_{sc}(L) = \frac{1}{N}\left|2\pi\sum_j A_j \delta\left(L - L_j\right)\right|^2 . \tag{34}$$

From the latter expression or from expression (28), the so-called *length spectrum* is revealed from the short length behavior of a given billiard's form factor. This behavior is clearly non-universal and can be used to identify the shortest POs with the largest contribution to the spectral density. This can be a genuine practical tool to gain some extra knowledge about the specific geometry of a cavity when one only knows part of its spectral response deduced from scattering experiments.

As an illustration, a length spectrum is shown in Figure 8 computed from the first 2000 eigenvalues of the truncated circle (see Figs. (4 and 6) with Dirichlet boundary conditions. As shown in section II A, this billiard is known to be chaotic in the strongest sense. A few POs among the shortest are indicated by arrows and are displayed in Fig. (9). Remark that the vast majority of periodic orbits contribute to the generic ergodic behavior described in section II C.

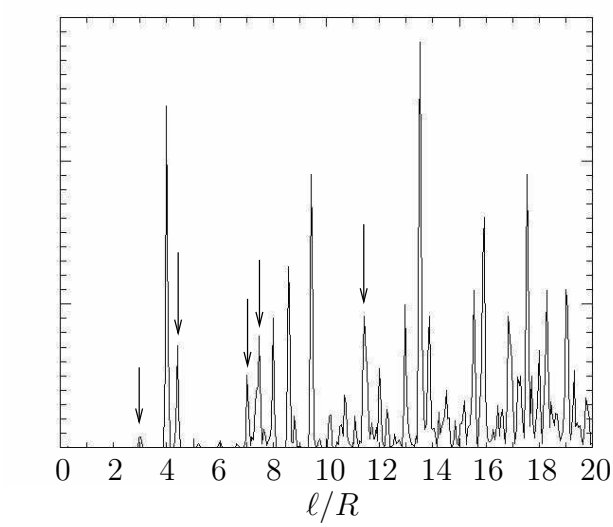

FIG. 8: The *length spectrum* or Fourier transform of the density of states $n(\kappa)$, for the eigenvalue problem (5) in the truncated chaotic billiard shown in Figs. 4 and 6. The *trace formula* permits to show that the length spectrum should have peaks at the period lengths of the periodic orbits. Arrows indicate lengths corresponding to the periodic orbits shown in figure 9.

Nonetheless, a special family of POs, namely the continuous family of diameters which survived the truncation, and constitute marginally unstable periodic orbits, are responsible for some of the high peaks at short length and thus also responsible for non-universal features of the long range spectral correlations as well as for the non-gaussian statistics of the eigenmode (b) shown in Fig. (6).

B. From Ballistic to Scattering Systems : point-like scatterers and diffractive orbits

In a billiard where one or more point-like scatterers are added, an approach similar to what has been described in the previous sections is feasible. In diffractive systems with point-like singularities, classical trajectories that hit those points can be continued in any direction. These can nonetheless be treated within the wave description by introducing an isotropic diffraction coefficient D, which fixes the scattering amplitude at each scatterer. In previous works [23, 24], this diffraction constant has been calculated (with the free Green's function in [24]) to yield:

$$\mathsf{D} = \frac{2\pi}{-\ln(ka/2) - \gamma + i\pi/2} \tag{35}$$

where γ is the Euler constant and a is a characteristic length which may be interpreted as the non-vanishing radius of an s-wave scattering disc [23].

With the help of this diffraction constant, a Dyson's formula can be written for the Green's function which is expanded in a multiple scattering series, which, in the presence of a point scatterer located at $\vec{s}$, reads:

$$G(\vec{r},\vec{r}\,') = G_0(\vec{r},\vec{r}\,') + G_0(\vec{r},\vec{s})\,\mathsf{D}\,G(\vec{s},\vec{r}\,') \tag{36}$$

where G_0 is the unperturbed Green's function of the bare billiard. If two consecutive scattering events are more distant than a wavelength, a semiclassical approximation for the unperturbed Green's function can be used, so that a semiclassical trace formula can be obtained for the perturbed billiard, which is based on POs and Diffractive periodic Orbits (DO) as well. These DOs are composed of closed orbits all starting and ending at the same scatterer. Hence the oscillating part of the modal density now includes DOs, yielding

$$\rho^{osc}(k) = \rho^{osc}_{PO}(k) + \rho^{osc}_{DO}(k) \tag{37}$$

where the term with the subscript PO is the corresponding part of the Gutzwiller trace formula (11) and the term with the subscript DO is a similar sum over all DOs.

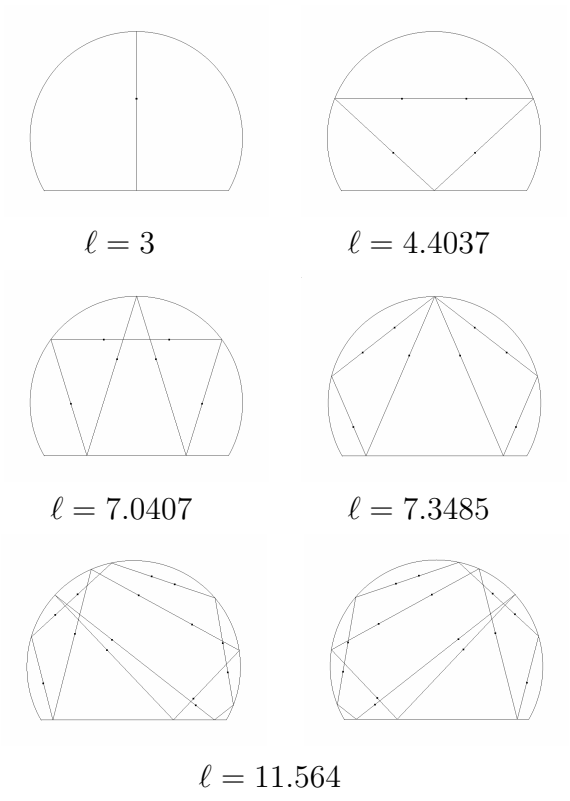

FIG. 9: A few periodic orbits whose periods (in units of R) correspond to peaks of the length spectrum shown in figure (8).

For instance, in a rectangular domain of area $\mathcal{A}$ with a single point scatterer, contributions from periodic orbits and diffractive orbits respectively read [25]:

$$\rho_{PO}^{osc} = \frac{\mathcal{A}}{\pi} {\sum_{PO}}' \sum_{r=1}^{\infty} \frac{k}{\sqrt{2\pi k r L_{PO}}} \cos(krL_{PO} - rn_{PO}\pi - \pi/4) \tag{38}$$

and

$$\rho_{DO}^{osc} = {\sum_{DO}}' \frac{L_{DO}}{\pi} \frac{\mathsf{D}}{\sqrt{8\pi k L_{DO}}} \cos(kL_{DO} - n_{DO}\pi - 3\pi/4) \tag{39}$$

where $\sum'$ denotes a sum over primitive periodic (diffractive) orbits of length L_{PO} (L_{DO}) and number of bounces n_{PO} (n_{DO}), and r is the number of repetitions. In formula (39) only leading order one-scattering events are included, repetitions or concatenations of primitive orbits of order ν being of order $\mathcal{O}(k^{-\nu/2})$ [25].

The problem of numerically calculating the eigenwavenumbers in the presence of a point scatterer in a rectangular billiard with Dirichlet boundary conditions has been solved for instance in [26, 27] and more recently revisited in [28] where the authors provide a comparison with experimental results in a two-dimensional microwave cavity.

An example of a length spectrum corresponding to a rectangular cavity with a single point scatterer is given in Figure 10. Here, the dimensions of the cavity in which we have performed our calculations are those of an actual microwave cavity used in our experiments, with perimeter $\mathcal{L} = 2.446\,\mathrm{m}$ and area $\mathcal{A} = 0.3528\,\mathrm{m}^2$. A large number of modes (approximately 12000) have been used so that the length resolution is excellent. To illustrate that such a length spectrum still is dominated by the POs of the empty cavity, the amplitude scale chosen in Figure 10 is such that the contributions of the DOs are much too small to be seen.

POs are easily identified on the length spectrum shown in Figure 10. At first sight, it could even seem that no other contribution can be seen as if the DOs were absent from it. Somehow, it could even be expected since no long range correlations are observed in the frequency spectrum thereby indicating that, if the DOs should contribute, especially at short lengths, they should only in a negligible way. This is what can be observed by closely inspecting a typical length spectrum for lengths smaller or of the order of the size of the cavity in the presence of a single point scatterer.

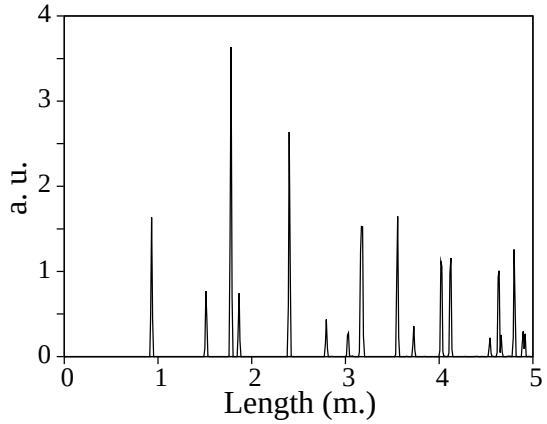

FIG. 10: Length spectrum computed in a a rectangular cavity with a single point scatterer. Approximately 12000 resonances have been used.

In Figure 11, the contributions of the DOs are displayed on the length range from 0 to 1.6 m using an enlarged scale for the amplitude of the peaks. Sticks with different styles indicate the lengths of the DOs (dotted) and POs (dashed) within this range.

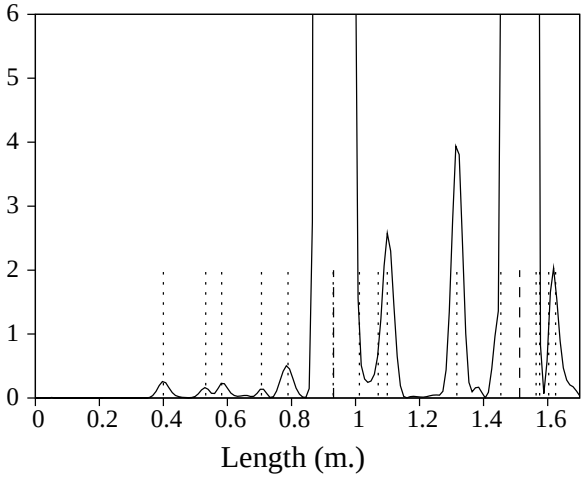

FIG. 11: Zoom ($\times 10^4$) of the length spectrum shown in Figure 10 on the length range from 0 to 1.6 m using an enlarged scale for the amplitude of the peaks : POs (dashed sticks), DOs (dotted sticks)

In [27], R. L. Weaver and the present authors proposed a heuristic way of semiclassically understanding the short and mid-range spectral correlations of rectangular billiards with point scatterers. In particular, a semiclassical prediction for the form factor in the universal regime was proposed. It corresponded to the typical two-point spectral correlations observed in such pseudo-integrable billiards and also produced the linear behavior of the spacing distribution at small spacings (known as the *level repulsion* which is typical of GOE spectra). At large spacings, however, the spacing distribution of spectra calculated in such rectangular billiards with point scatterers, decreases exponentially thus behaving like the so-called *Poisson* distribution generically observed for uncorrelated spectra associated to integrable billiards (such as the rectangle) [16].

The argument proposed in [27] is now briefly summarized. First, one has to acknowledge that the wave problem associates a finite size of the order of the cross section σ (here a length) to the point scatterer. From the expression (35) of the diffraction constant, one can show [28] that, apart from a logarithmic correction, the scattering cross section essentially scales as the wavelength,

$$\sigma = |\mathsf{D}|^2/4k \tag{40}$$

thus making the scatterer practically equally efficient at all frequencies in a given band. Thus, in a coarse-grained way obtained, for instance, by averaging the modal density over a small k-interval, the orbits which are effectively scattered at lengths much larger than the shortest DOs, are those which meet a small disk of diameter σ centered on the scatterer. The rate at which a typical ray hits this disk is given by a Sabine-like expression

$$\Gamma = \frac{\pi\sigma}{\pi\mathcal{A}} \tag{41}$$

One then evaluates the form factor by considering it results from two contributions: one from the original POs of the bare rectangle which have not met the disk at length L, and another one from *new* POs which have met the disk. For the first *regular* part of the form factor, the fraction of orbits which have survived decays like $\exp(-\Gamma L)$, thus yielding

$$K^{reg}(L) \approx K^{rect}(L)\exp(-\Gamma L) = \exp(-\Gamma L) \tag{42}$$

(where $K^{rect}(L) = 1$ yields *Poisson* statistics for uncorrelated spectra, see, for instance, Ref. [29]), whereas, for the *scattered* part, the probability of having met the disk at length L behaves like $1 - \exp(-\Gamma L)$ thus yielding

$$K^{scat}(L) \approx 2\frac{L}{L_H}\left[1 - \exp(-\Gamma L)\right] \quad \text{if} \quad L \ll L_H \tag{43a}$$

$$\approx \left[1 - \exp(-\Gamma L)\right] \quad \text{if} \quad L \gg L_H\,, \tag{43b}$$

where the proliferation of scattered periodic orbits was assumed to follow the same sum rule as the POs of a genuinely chaotic billiard (following an argument introduced in [30]). In a 2D billiard with area $\mathcal{A}$, $L_H = \mathcal{A}k$ so that $\Gamma L_H = |\mathsf{D}|^2/4$ is practically a constant in a given frequency band, therefore leading to a long length (i.e. $L \gg \Gamma^{-1}$) behavior of the form factor very similar to the one of chaotic systems displaying level repulsion. At shorter lengths (i.e. $L \ll \Gamma^{-1}$), $K(L) = K^{reg}(L) + K^{scat}(L)$ is practically unity like $K^{rect}(L)$, therefore leading to an absence of long-range spectral correlations. This was analytically demonstrated by Bogomolny, Gerland and Schmit [31] who used the fact that the eigenvalues of such singular billiards can be considered as the zeroes of random meromorphic functions with a large number of poles, when these poles are independent random variables.

If the billiard in which a point scatterer is added is already chaotic, Bogomolny, Lebœuf and Schmit have shown, by using both a random matrix argument and a semiclassical approach, that the spectral correlations are essentially not modified with respect to those of the bare chaotic billiard [32]. In a certain way, diffractive orbits cannot randomize more a system which is already fully chaotic.

IV. CONCLUSION

In the present chapter we have tried to provide a self-contained introduction to the semiclassical approach for the Helmholtz equation in complex systems known as chaotic billiards. These systems are paradigms of wave cavities where the chaotic ray motion of the geometrical limit has implications on the spectral response and on the distribution of wavefunctions. We have introduced the Trace formula, yielding the modal density in terms of a sum over the unstable Periodic Orbits of the billiard, and given a particular emphasis on its applications in spectral and spatial correlations. Its connection with Random Matrix theory has been discussed. To bridge the gap between chaotic billiards and scattering systems, we have also presented how the spectral correlations of billiards in the presence of a point scatterer can be influenced by periodic Diffractive Orbits, leading to level repulsion even though the unperturbed cavity is not chaotic.

Acknowledgments

We wish to thank Valérie Doya for useful criticism and careful reading of the manuscript.

[1] G. Tanner and N. Søndergaard, "Wave chaos in acoustics ans elasticity", J. Phys. A: Math. Theor. **44**, R443 (2007).
[2] F. Mortessagne, O. Legrand, D. Sornette, "Transient chaos in room acoustics", Chaos **3**, 529 (1993).
[3] F. Mortessagne, O. Legrand, D. Sornette, "Role of the absorption distribution and generalization of exponential reverberation law in chaotic rooms", J. Acoust. Soc. Am. **94**, 154 (1993).

[4] M. C. Gutzwiller, *Chaos in Classical and Quantum Mechanics*, (Springer-Verlag, New-York, 1991).
[5] M. V. Berry and K. E. Mount, "Semiclassical approximations in wave mechanics", Rep. Prog. Phys. **35**, 315 (1972).
[6] E. B. Bogomolny and J. P. Keating, "Gutzwiller's Trace Formula and Spectral Statistics: Beyond the Diagonal Approximation", Phys. Rev. Lett. **77**, 1472 (1996).
[7] H.-J. Stöckmann *Quantum Chaos: An Introduction*, Cambridge University Press, Cambridge, UK (1999).
[8] M. C. M. Wright and C. J. Ham, "Periodic orbit theory in acoustics: spectral fluctuations in circular and annular waveguides", J. Acoust. Soc. Am. **121**, 1865 (2007).
[9] M. C. M. Wright , chapter XX of the present book.
[10] M. V. Berry, "Some Quantum-to-Classical Asymptotics", in *Chaos and Quantum Physics*, M.-J. Giannoni, A. Voros and J. Zinn-Justin (Eds.), Les Houches 89, Session LII (North-Holland, Amsterdam, 1991).
[11] A. Voros, "Semi-classical ergodicity of quantum eigenstates in the Wigner representation", Lect. Not. Phys. **93**, 326-333 (1979).
[12] M. V. Berry, "Regular and irregular semiclassical wavefunctions", J. Phys. A:Math. Gen. **10**, 2083-1091 (1977).
[13] M. V. Berry, "Semiclassical mechanics of regular and irregular motion", in *Chaotic behaviour of deterministic systems*, R. H. G. Helleman, and G. Ioss (Eds.), Les Houches 82, Session XXXVI (North-Holland, Amsterdam, 1983).
[14] M. Srednicki, and F. Stiernelof, "Gaussian fluctuations in chaotic eigenstates", J. Phys. A:Math. Gen. **29**, 5817-5826 (1996).
[15] F. Haake, *Quantum Signatures of Chaos*, (Springer-Verlag, Berlin Heidelberg, 1991).
[16] R. L. Weaver, chapter XX of the present book.
[17] E. J. Heller, "Wave packet dynamics and quantum chaology", in *Chaos and Quantum Physics*, M-J. Giannoni, A. Voros, and J. Zinn-Justin (Eds.), Les Houches 89, Session LII (North-Holland, Amsterdam, 1991).
[18] V. Doya, O. Legrand, F. Mortessagne, and Ch. Miniatura, "Speckle statistics in a chaotic multimode fiber", Phys. Rev. E **65**, 056223 (2002).
[19] E. Bogomolny, "Smooth wavefunctions of chaotic quantum systems", Physica D **31**, 169-189 (1988).
[20] E. Vergini, chapter XX of the present book.
[21] D. Delande, "The semiclassical approach for chaotic systems", in *Waves and imaging through complex media*, P. Sebbah (Ed.), International Physics School, Cargèse, 1999 (Kluwer Academic Publishers, Amsterdam, 2001).
[22] O. Bohigas, M. J. Giannoni, and Ch. Schmit, "Characterization of chaotic spectra and universality of level fluctuation laws", Phys. Rev. Lett. **52**, 1 (1984).
[23] P. Exner and P. Šeba, "Point interactions in two and three dimensions as models of small scatterers", Phys. Lett. A **222**, 1 (1996).
[24] S. Rahav and S. Fishman, "Spectral statistics of rectangular billiards with localized perturbations", Nonlinearity **15**, 1541 (2002).
[25] N. Pavloff and C. Schmit, "Diffractive orbits in quantum billiards", Phys. Rev. Lett. **75** 61 (1995); erratum **75** 3779 (1995).
[26] R. L. Weaver and D. Sornette, "Range of spectral correlations in pseudointegrable systems: Gaussian-orthogonal-ensemble statistics in a rectangular membrane with a point scatterer", Phys. Rev. E **52** 3341 (1995).
[27] O. Legrand, F. Mortessagne and R. L. Weaver, "Semiclassical analysis of spectral correlations in regular billiards with point scatterers", Phys. Rev. E, **55** 7741 (1997).
[28] D. Laurent, O. Legrand and F. Mortessagne, "Diffractive orbits in the length spectrum of a two-dimensional microwave cavity with a small scatterer", Phys. Rev. E, **74** 046219 (2006).
[29] M. V. Berry and M. Tabor, "Level clustering in the regular spectrum", Proc. R. Soc. London Ser. A **356**, 375 (1977)
[30] N. Argaman, Y. Imry and U. Smilansky, "Semiclassical analysis of spectral correlations in mesoscopic systems ", Phys. Rev. B **47**, 4440 (1993).
[31] E. Bogomolny, U. Gerland and C. Schmit, "Singular statistics", Phys. Rev. E **63** 036206 (2001).
[32] E. Bogomolny, P. Lebœuf and C. Schmit, "Spectral Statistics of Chaotic Systems with a Pointlike Scatterer", Phys. Rev. Lett. **85**, 2486 (2000).